

SHORT TERM MOBILITY PROGRAM 2010

Proponente: Romolo Marcelli

Fruitore: Emanuela Proietti

Istituto di afferenza del Fruitore: ISTITUTO PER LA MICROELETTRONICA E MICROSYSTEMI

Istituzione ospitante: California Institute of Technology –Pasadena USA

Titolo del programma: Biological Impact and Mechanism for low intensity millimeter-waves interactions with tissue

My Short Term Mobility activity in the period 23/10-20/11/2010 was focused on the study of the Specific Absorption Rate (SAR) in leech ganglion cells exposed with low power millimeter waves. This work has been done on the biological set-up studied by Dr. Peter H. Siegel (Caltech-JPL laboratories) and Dr. Viktor Pikov from the Huntington Medical Research Institute in the MOORE Laboratories of California Institute of Technology located in Pasadena.

Abstract

Biological effects of millimeter wave region of the electromagnetic spectra, extending from 30 GHz to 300 GHz in term of frequencies, have gained a restoring interest in research in the recent years. This radiation is produced by many man-made sources, it is officially used in non complementary medicine in many countries against a variety of diseases and in the near future will find applications in high resolution and high speed wireless communication technologies [1].

Dr. P. H. Siegel and Dr. Pikov have evidenced in several experiments the impact of millimeter waves on individual neuronal cells at the microscopic level. In the course of these investigations, they found evidence for transient membrane depolarization in epithelial and neuronal cell lines [2] and altered neuronal firing in cortical cells at RF power levels [3].

In order to quantify the power introduction into the cell layer, dosimetric calculations using the finite differences time domain method in the program Quickwave 5.0 have been performed to access the field and so the specific absorption rate (SAR).

Introduction

Millimeter wave radiation is produced by many sources, including medical equipment as well as a diverse assortment of other electronic devices within our living and working environments. Sufficiently intense MMW radiation can cause heating of materials with finite conductivity, including biological tissues [4].

The study of effects induced by Millimeter wave radiation is related to the problem of the interaction between electromagnetic fields and biological systems. This issue is of interest because of fundamental scientific curiosity, potential medical benefits, and possible human health hazards. The latter problem has been studying for decades leading to a big deal of papers indicating potential dangerous effects.

The specific biological responses to radiation are generally related to the rate of energy absorption. The rate and distribution of radiation energy absorbed depend strongly on the frequency, intensity and orientation of the incident fields as well as the material size and the constitutive properties of the tissues (dielectric constant and conductivity). At frequencies above 1 MHz, absorption of RF radiation is commonly described in terms of the specific absorption rate (SAR), which is a measure of the rate of energy deposition per unit mass of body tissue and is usually expressed in units of watts per kilogram (W/kg).

A number of well-established biological effects and adverse health effects from acute exposure to intense RF radiation have been documented [5],[6]. For the most part, these effects relate to localized heating or stimulation of excitable tissue from intense MMW radiation exposure.

The debate is still open, even if several points have been fixed. The action of high-levels fields is well-known and has led to the definition of international safety standards by International Commission of Non-Ionizing Radiation Protection (ICNIRP) in 1998 [7].

However, the safety of exposure to long-term, low-level RF radiation remains controversial and the risk of development of cancer remains a primary public health concern.

Meantime, projects on low power level irradiation have been no more funded in the recent years. Several investigations have noted significant impact on neuronal activity from modest level millimeter wave exposures (40-130 GHz, 1-100 mW/cm², seconds to minutes) that are not much higher than the Federal Communications Commission-established maximum permissible exposure (MPE) limits of 1 mW/cm² for 6 minutes in the 30-300 GHz frequency regime. Moreover this limit is mainly related to a problem of temperature increase in the biological tissue but the capability of low power millimeter waves to induce both excitatory and inhibitory responses in neurons as well as the potential to induce changes in membrane permeability is insufficient to cause dramatic changes in the local thermal environment. This has moved our investigation on a more detailed look at the energy coupling occurring at the cellular level. Recent studies on the prevalence and role of macromolecule-bound water, particularly inside and adjacent to the cellular membrane, point to strong specific absorption in the millimeter wave band [8-11].

Dr. Pikov and Dr. Siegel are working on several experiments, performed in vitro and ex vivo, which address the impact of millimeter waves on individual cells at the microscopic level. They have found evidence for transient membrane depolarization in epithelial and neuronal cell lines and altered neuronal firing at RF power levels well below the MPE.

In order to quantify and reliably evaluate the stress imposed on the living cells, it is necessary to determine the SAR within a monolayer of cells covered by culture medium in a cell container performing a dosimetric calculations to quantify the power introduction into the cell layer. The numerical calculations have been done using the finite-differences time-domain method as implemented in the program Quickwave.

A detailed geometric model of the sample container and realistic dielectric properties of the materials are used to obtain reliable SAR values at 60 GHz.

Field Exposition Experiments

In this activity the leech ganglion cells were exposed to 60 GHz millimeter radiation. The cells were cultivated in a culture media in a container as in Fig. 1.

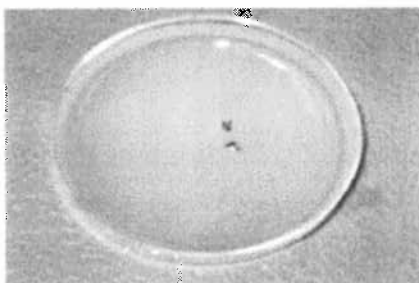


Fig. 1 Cells sample and culture media container.

The container is made of polystyrene and the cells are full immersed in the culture media fixed to a paraffin layer . The dimension of the different layers are in Tab. 1

Layer	Thickness	Diameter
Culture media (SALINE)	1 mm	5 cm
Paraffin	2 mm	5 cm
Polystyrene	0.75 mm	5 cm

Saline
Paraffin
Polystyrene

Tab 1. Dimension of the leech ganglion culture container.

The cells are exposed by single mode linearly polarized RF power supplied by an open ended waveguide placed below the sample. The rectangular waveguide with 3.8x1.9 mm aperture can be positioned above or below the sample and the power directed perpendicular to the plane of the sample for a more uniform irradiation of the area occupied by the cells. The firing rate and the cells potentials were measured by patch clamp [2], [3].

The problem of this set up is the characterization of the power density and specific absorption rate (SAR) applied to the sample. Since most culture media are water based, and the RF absorption coefficient, α , in pure water at 60 GHz for example is approximately 50 cm⁻¹ with a refractive index close to 4, a variation of a few microns in the fluid depth between the sample and the air filled waveguide causes substantial changes in coupling of the incident power [2].

Dosimetric Calculations

We simulated two different conditions of the set-up:

- Up irradiation with the waveguide positioned above the sample in two positions:
 - o far field (6 mm)
 - o near field (0.5 mm)
- Down irradiation with the waveguide positioned below the sample in two positions:
 - o far field (6 mm)
 - o near field (0.5 mm)

The dielectric characteristics of the structure must be defined carefully in order to determine an appropriate physical model for a reliable computation of the SAR. They are listed in the Tab.2 [12]

Medium	Relative permittivity	Loss tangent	Ionic conductivity	Density
--------	-----------------------	--------------	--------------------	---------

Free Water	16.11-24.17j	1.5	0	1
Polystyrene	2.56-0.0003j	0.0001	0	1.05
Saline (Culture medium)	15.19-22.41j	1.48	1.5	1
Paraffin	2.27-0.0005j	0.0002	0	0.8

Tab. 2 Material properties used for the simulations at 60 GHz [12].

In the following Fig. 2 is represented the the computer model (Quickwave 5.0) with the waveguide above the cells container:

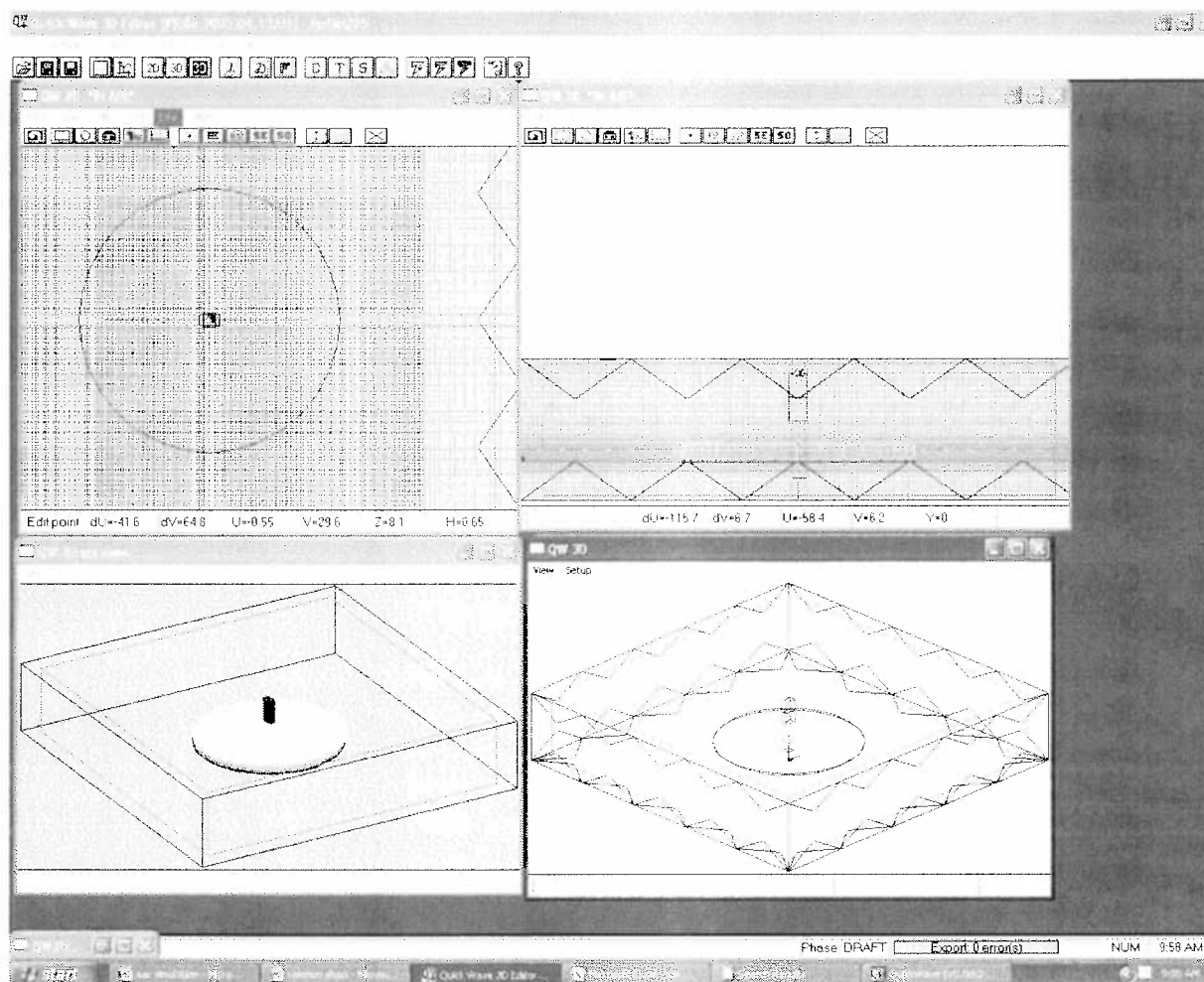
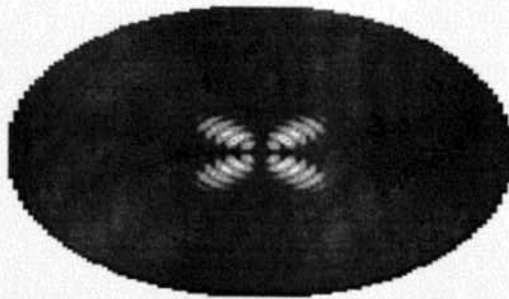
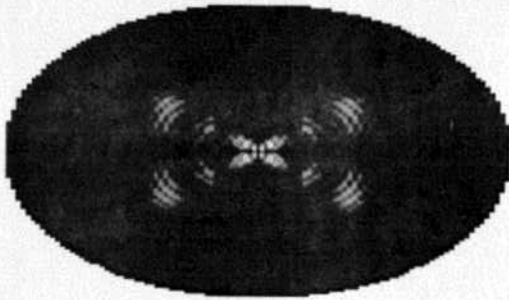
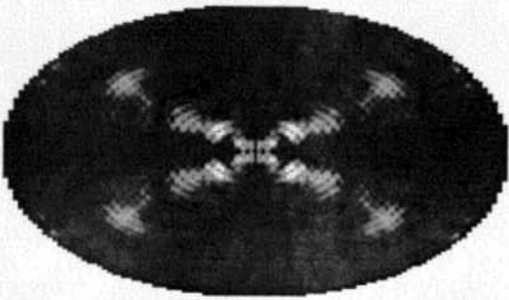


Fig. 2 Model of the up irradiation in far field condition (6 mm between waveguide and saline solution).

The calculated SAR distribution in the saline solution, in the paraffin and in the polystyrene are the following represented in Tab.3 :

Level	Distribution	SAR up far field
Saline		Max 1.05 W/kg
Paraffin		Max 3 W/kg
Polystyrene		Max 2.59 W/Kg

Tab.3 Results of the SAR distribution in the different layers with up irradiation and far field

In the following Fig.2 is represented the power flux (Poynting vector $\frac{1}{2} E_y \times H_x$) from the waveguide to the different layers in the central point:

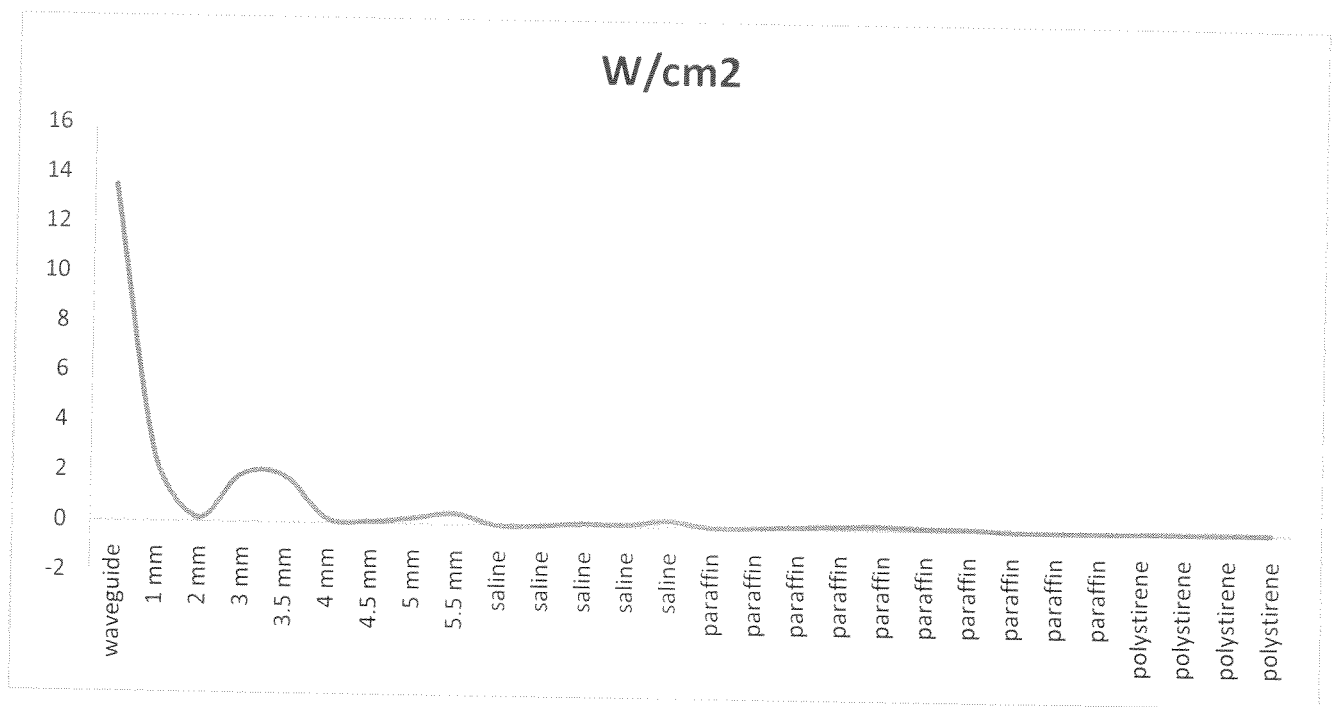


Fig.3 Power distribution in the central point from the waveguide to the sample (far field from up 6mm distance)

In the next Fig.4 and Fig.5 the dissipated power and SAR in the center of the sample:

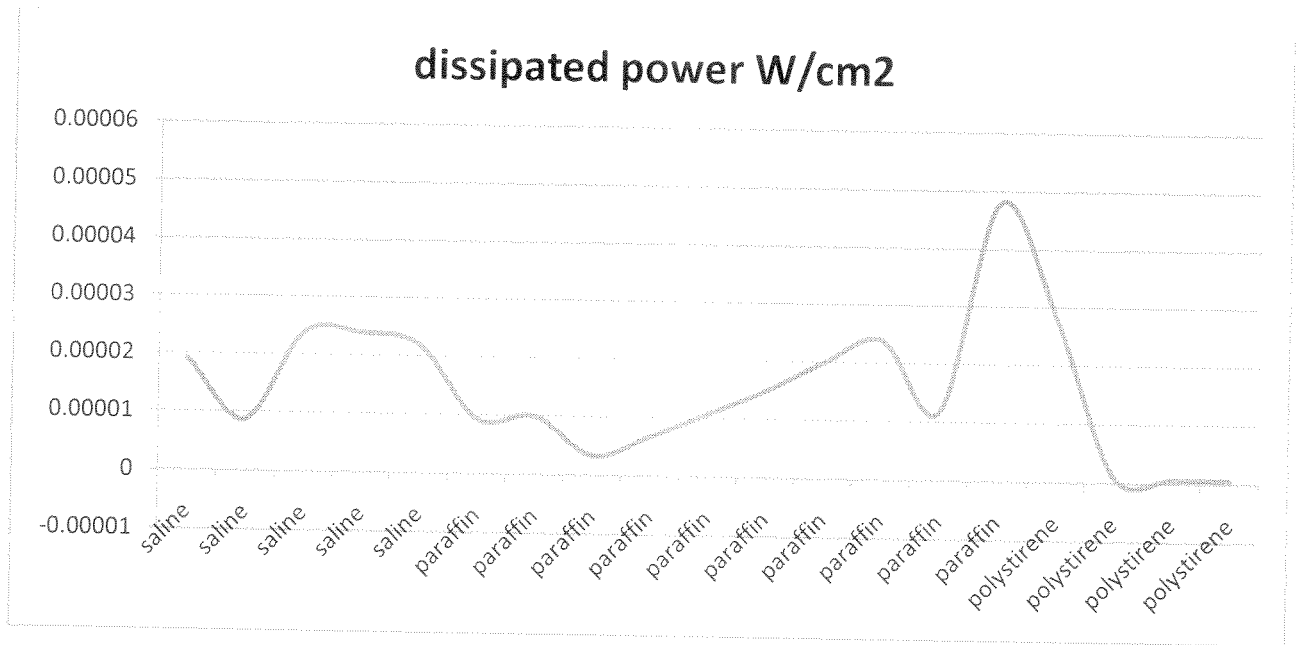


Fig.4 Dissipated power in the central point of the sample (far field from up 6 mm distance)

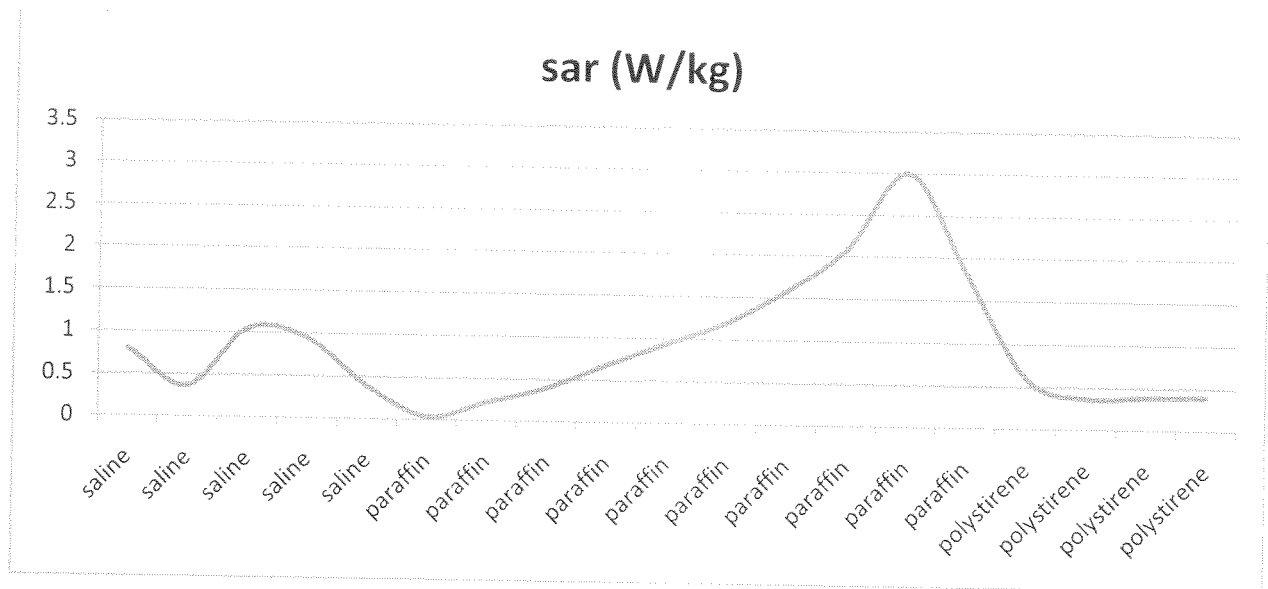


Fig.4 SAR value in the center of the sample(far field from up 6 mm distance).

In the following Fig. 5 is represented the the computer model (Quickwave 5.0) with the waveguide below the cells container:

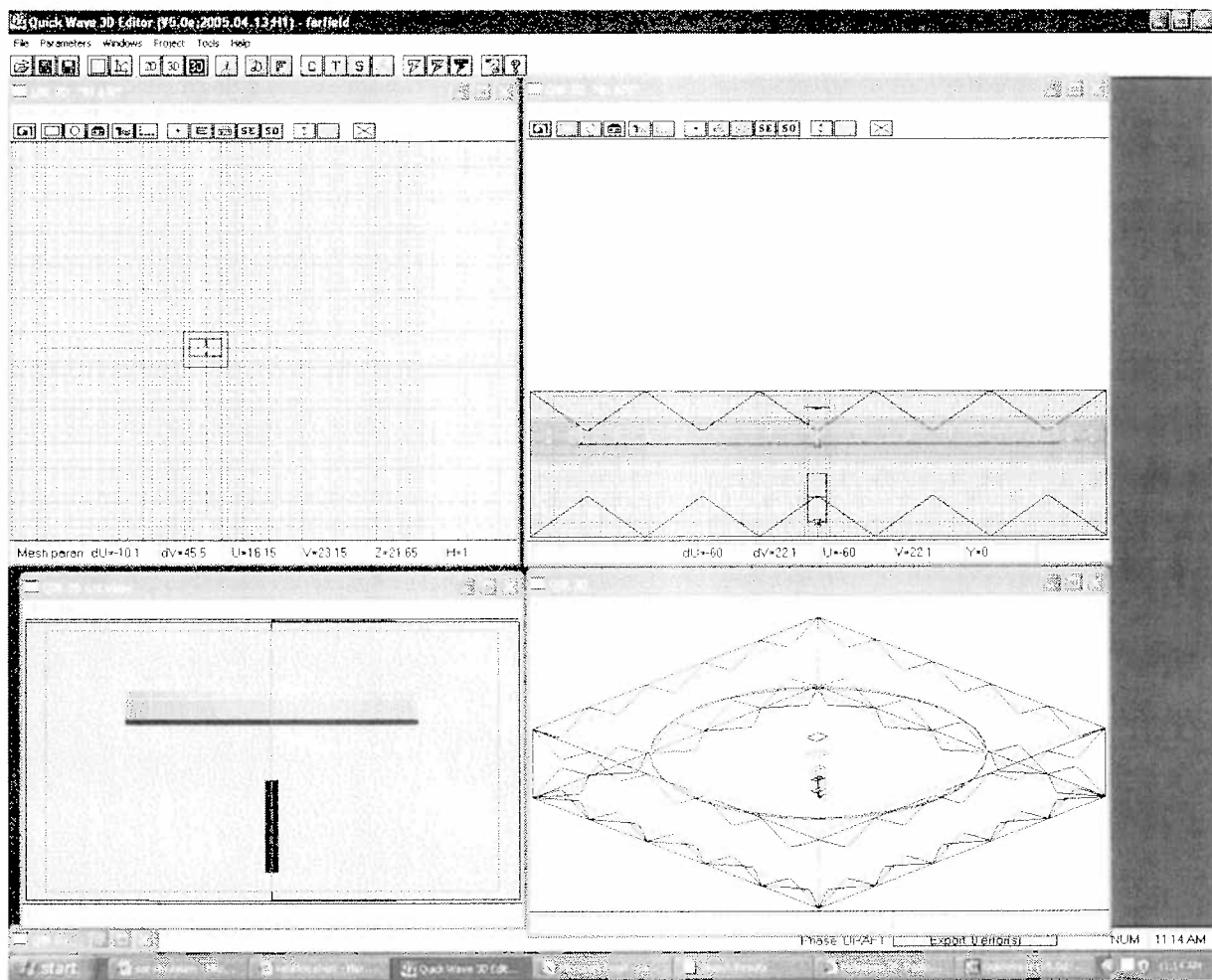
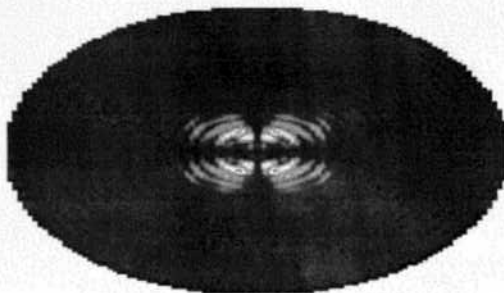
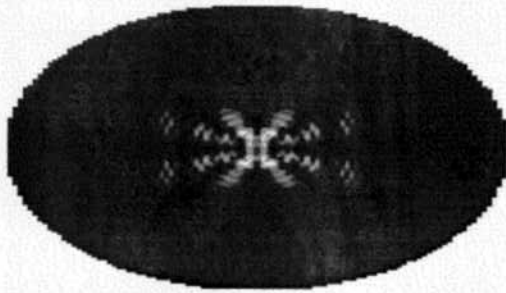
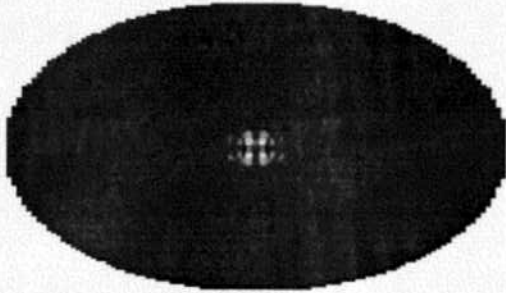


Fig. 5 Model of the down irradiation in far field condition (6 mm between waveguide and polystyrene).

The calculated SAR distribution in the saline solution, in the paraffin and in the polystyrene are the following represented in Tab.4:

Level	Distribution	SAR down far field
Saline		Max 1 W/kg

Paraffin		Max 2.56 W/kg
Polystyrene		Max 0.57 W/kg

Tab.4 Results of the SAR distribution in the different layers with down irradiation and far field

In the following Fig.6 is represented the power flux (Poynting vector $\frac{1}{2} E_y \times H_x$) from the waveguide to the different layers in the central point:

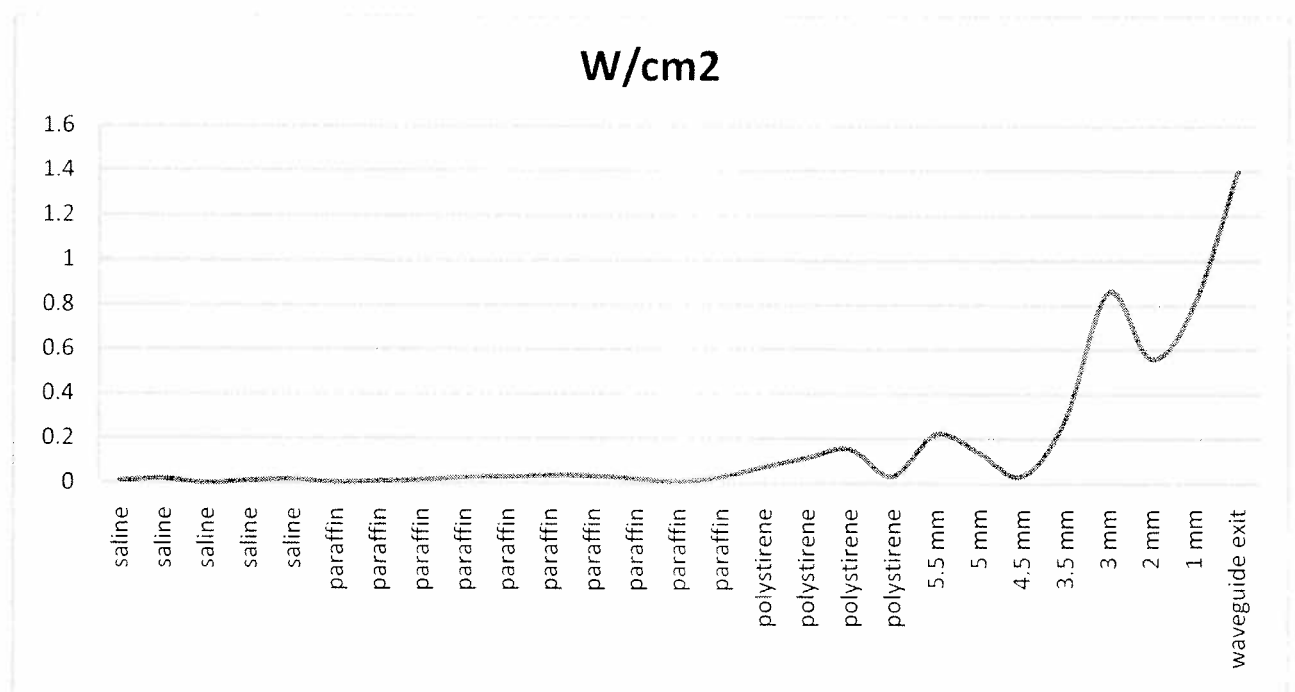


Fig.6 Power distribution in the central point from the waveguide to the sample (far field from down 6mm distance)

In the next Fig.7 and Fig.8 the dissipated power and SAR in the center of the sample:

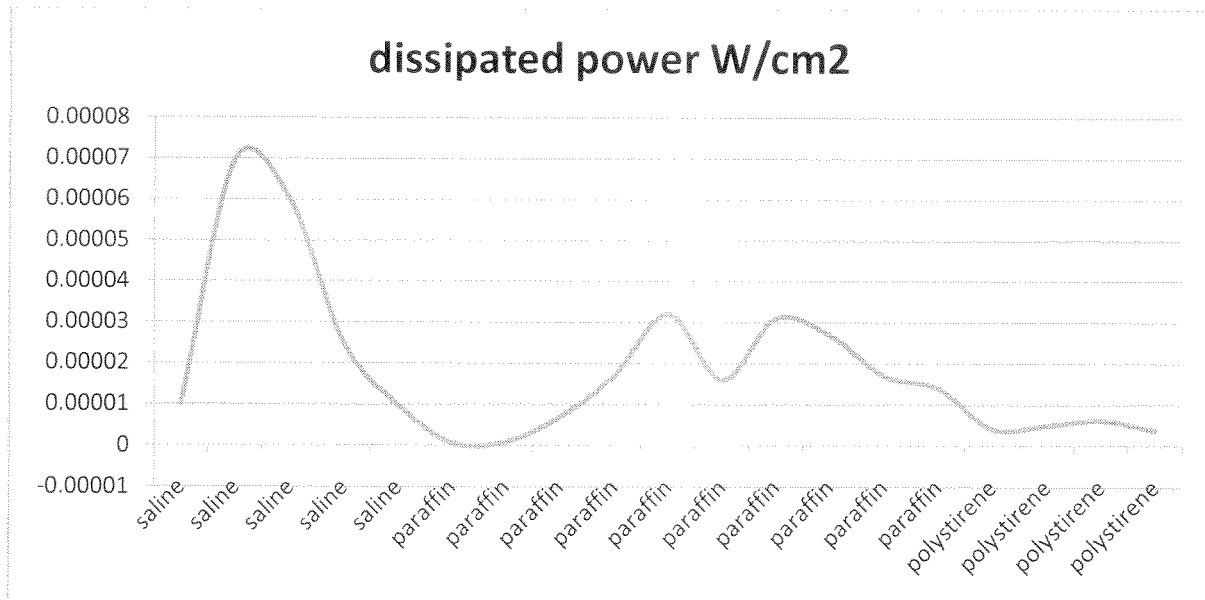


Fig.7 Dissipated power in the central point of the sample (far field from down 6 mm distance)

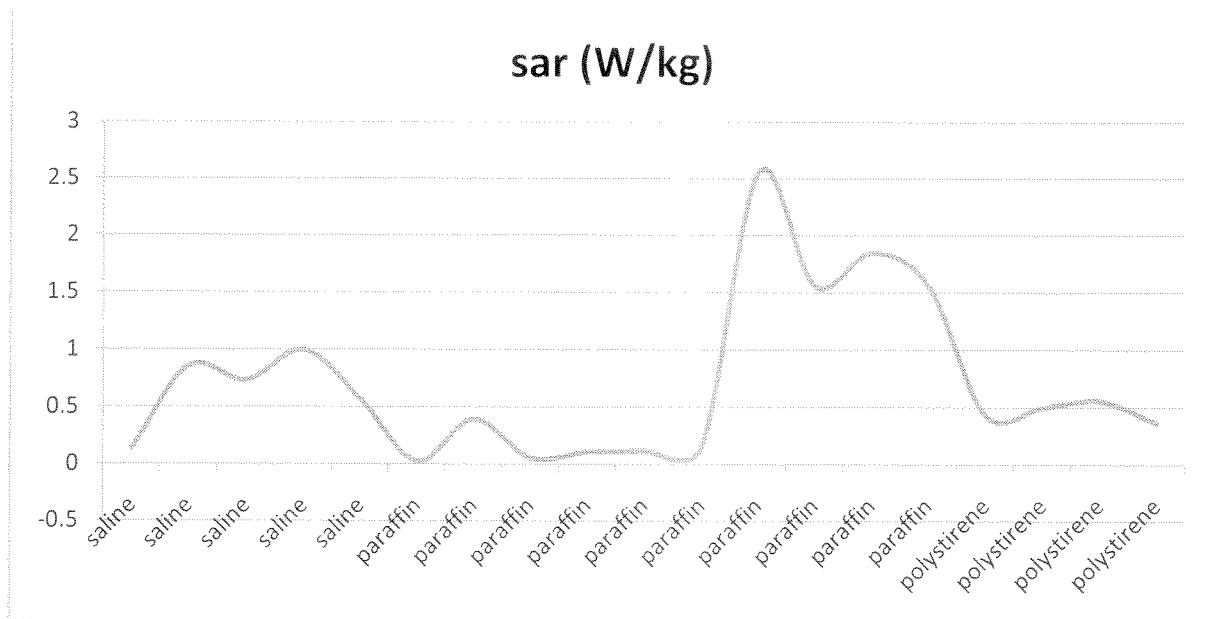
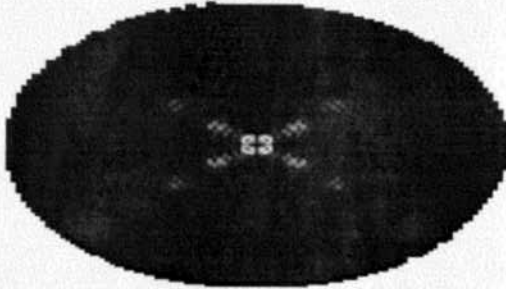
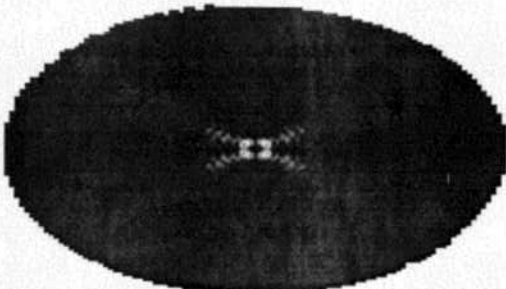
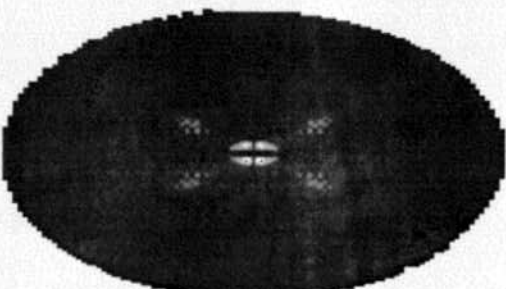


Fig.8 SAR value in the center of the sample (far field from down 6 mm distance).

The same simulations have been done in near field condition (distance 0.5 mm).

Near field from up:

Level	Distribution	SAR up near field
Saline		Max 18 W/kg
Paraffin		Max 12 W/kg
Polystyrene		Max 4.2 W/Kg

Tab.3 Results of the SAR distribution in the different layers with up irradiation and near field

In the following Fig.9 is represented the power flux (Poynting vector $\frac{1}{2} E_y \times H_x$) from the waveguide to the different layers in the central point:

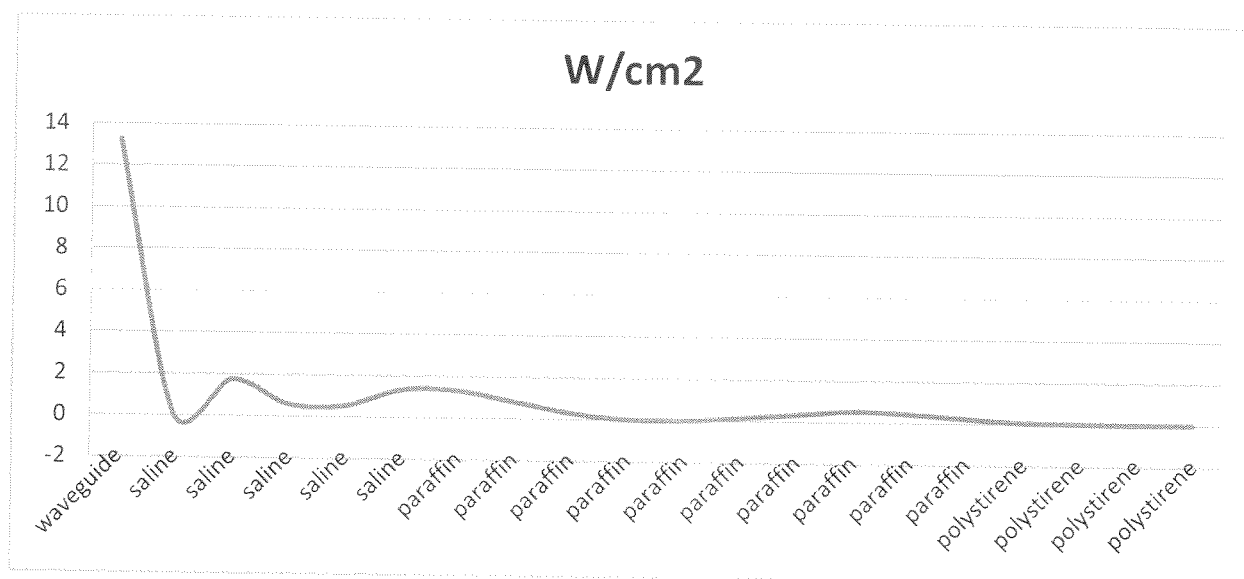


Fig.9 Power distribution in the central point from the waveguide to the sample (near field from up 0.5 mm distance)

In the next Fig.10 and Fig.11 the dissipated power and SAR in the center of the sample:

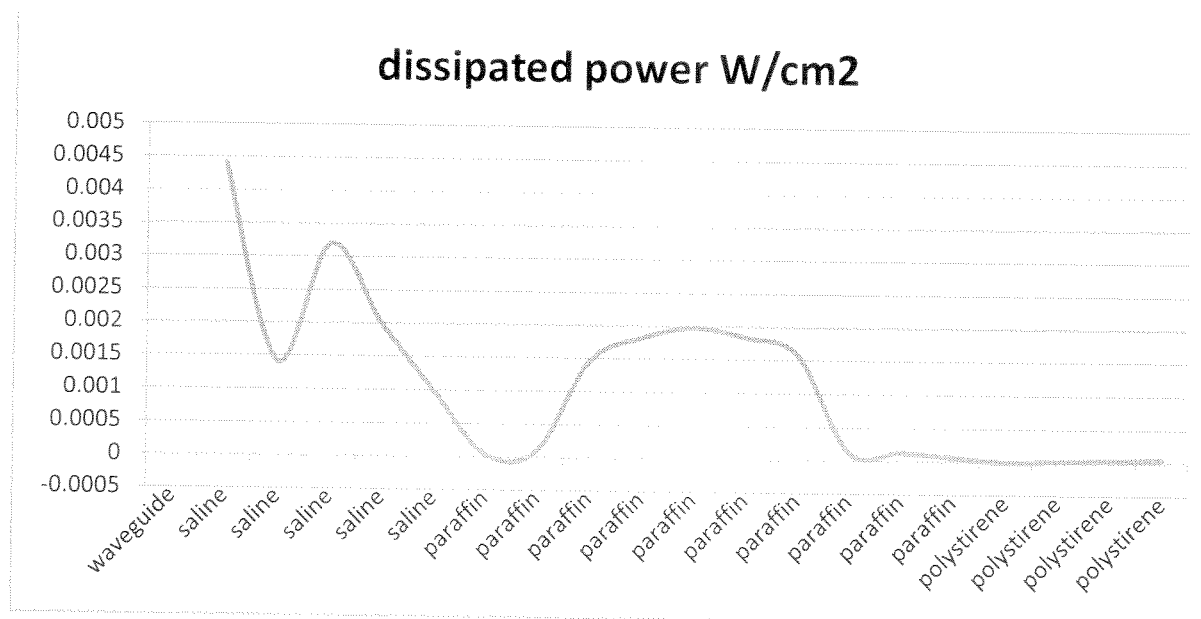
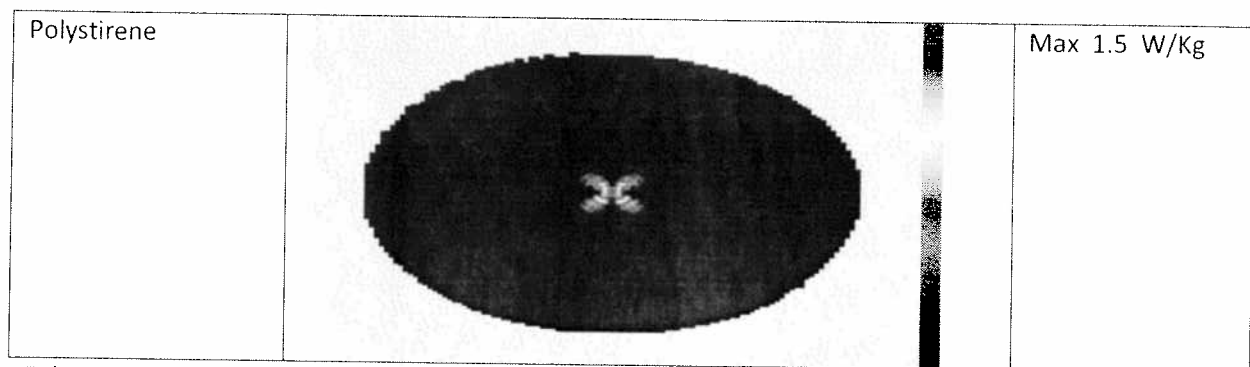


Fig.10 Dissipated power in the central point of the sample (near field from up 0.5 mm distance)



Tab.4 Results of the SAR distribution in the different layers with down irradiation and near field

In the following Fig.12 is represented the power flux (Poynting vector $\frac{1}{2} E_y \times H_x$) from the waveguide to the different layers in the central point:

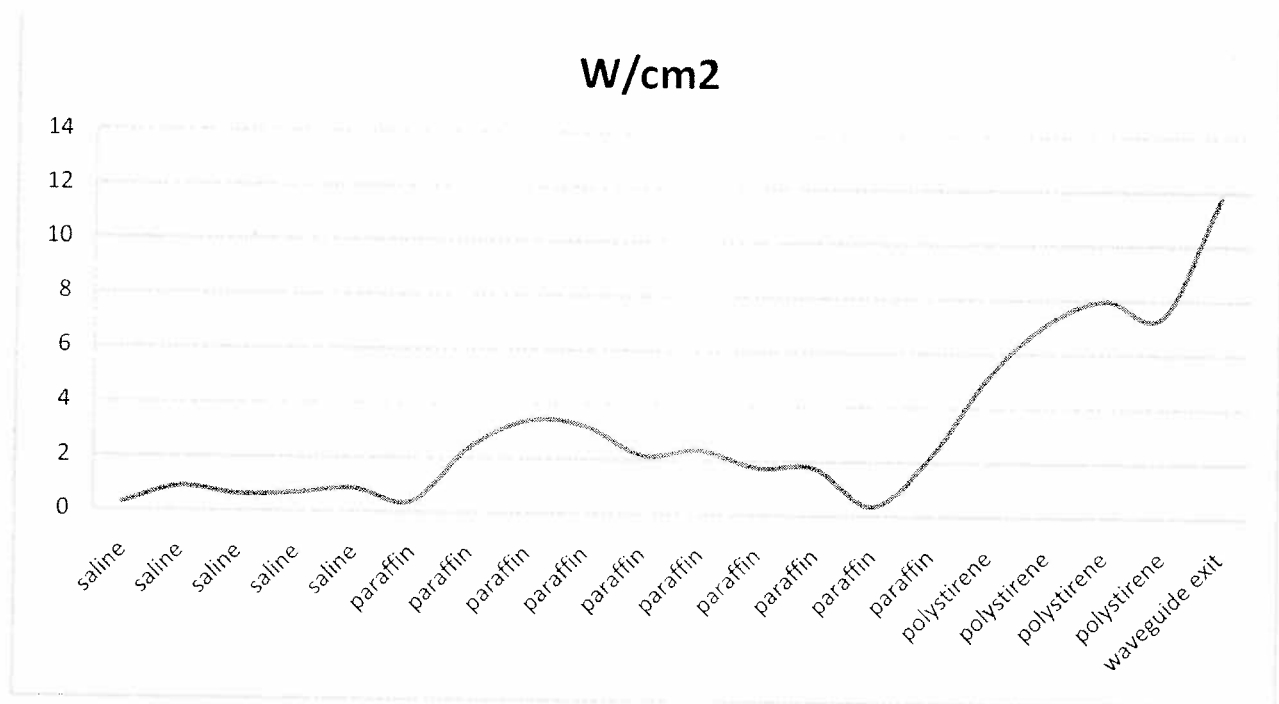


Fig.12 Power distribution in the central point from the waveguide to the sample (near field from down 0.5 mm distance)

In the next Fig.13 and Fig.14 the dissipated power and SAR in the center of the sample:

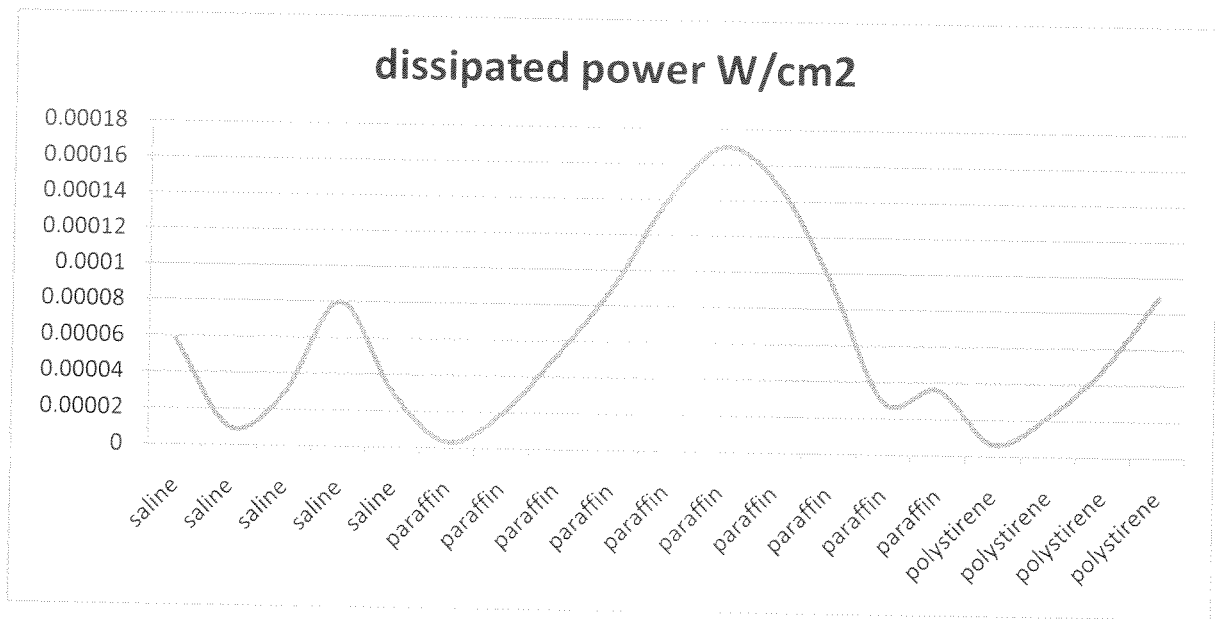


Fig.13 Dissipated power in the central point of the sample (near field from down 0.5 mm distance)

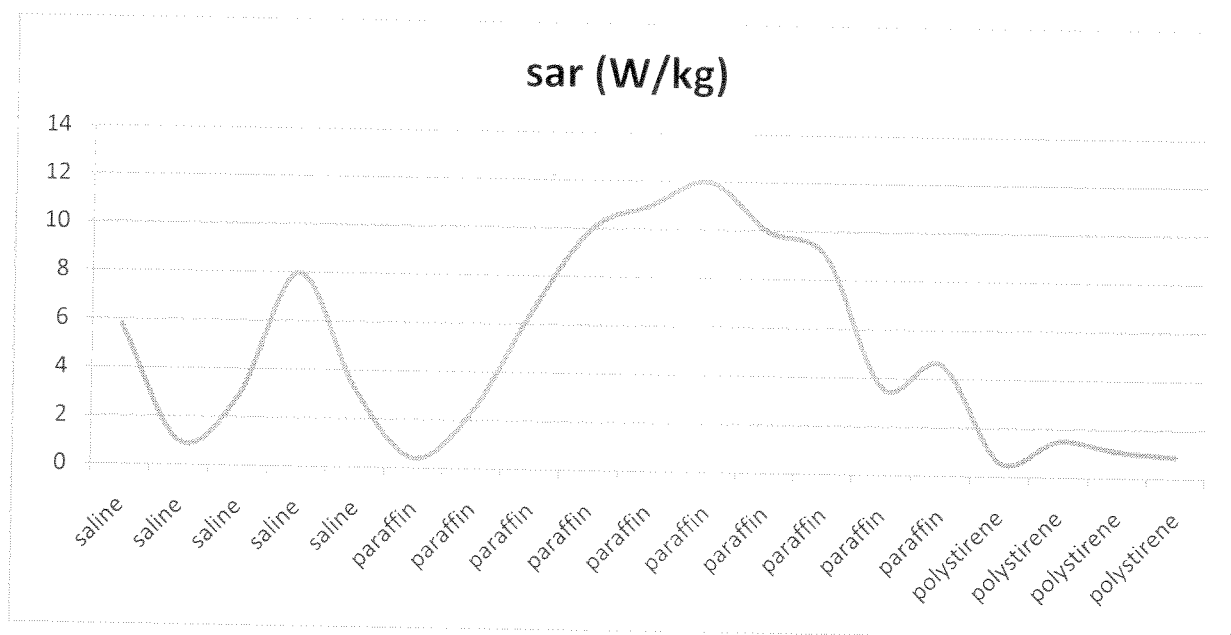


Fig.14 SAR value in the center of the sample(near field from down 0.5 mm distance).

Conclusions and future development

The dosimetric calculations show that the RF power density is related to the depth of the fluid, the dielectric interfaces encountered along the RF path and the distance of the sample from the waveguide

and the irradiation path. In the next Fig.15 and 16 are represented the SAR from the 4 configurations and the dissipated power:

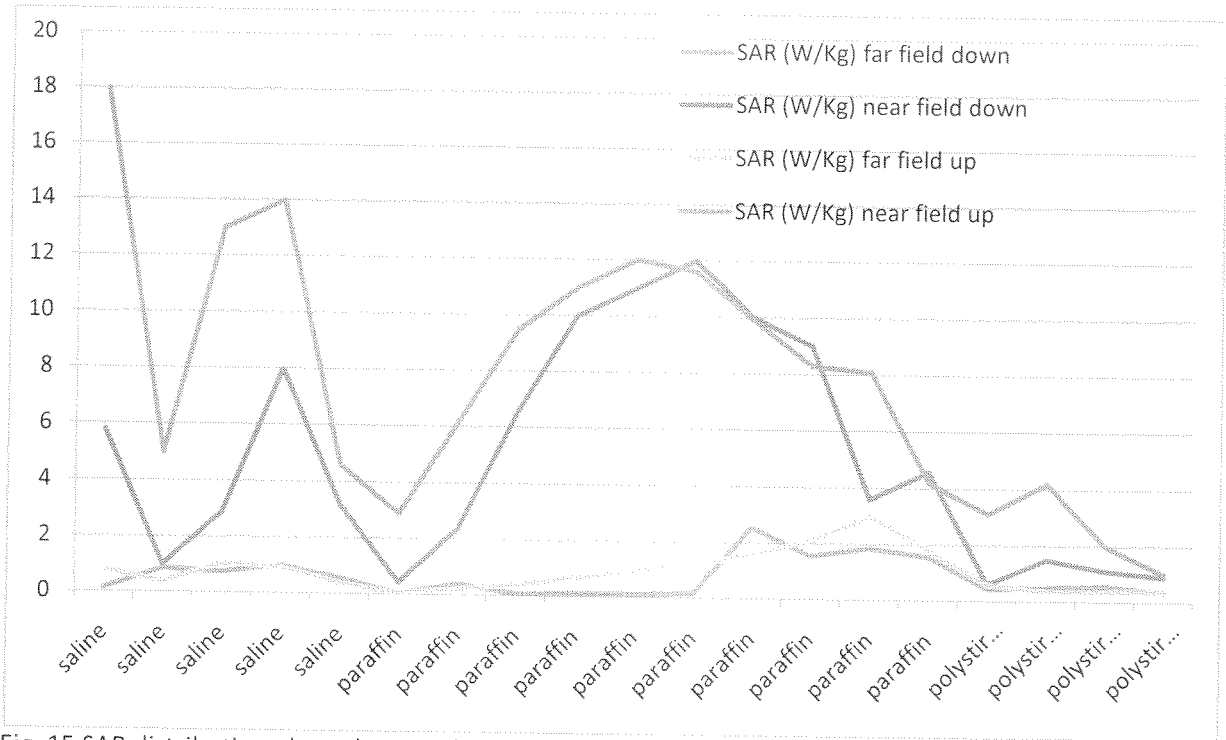


Fig. 15 SAR distribution along the sample for the simulated fields

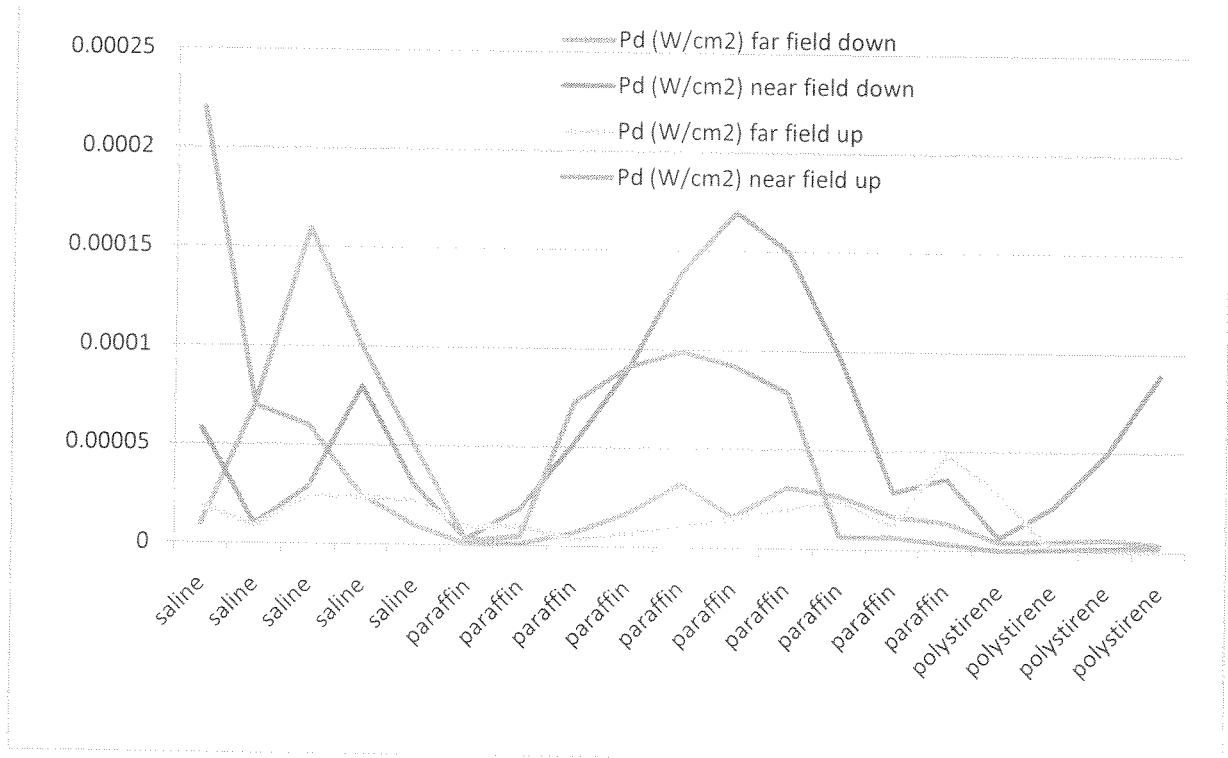


Fig. 16 Dissipated power distribution along the sample for the simulated fields

The future development of this collaboration will be the joint design and realization of a biocompatible detector for this power levels.

Acknowledgments

I would like to acknowledge Dr. Romolo Marcelli and Dr. Peter Siegel for the technical support, Dr. Peter Siegel for letting me attending the Caltech laboratory and biological set up and Dale Yee for the logistic support.

References

- [1] A. Ramundo Orlando "Effects of Millimeter Waves Radiation on Cell Membrane - A Brief Review" *Journal of Infrared, Millimeter and Terahertz Waves* DOI: 10.1007/s10762-010-9731-z (2010)
- [2] V. Píkov et al. "THz in Biology and Medicine: Towards Quantifying and Understanding the Interaction of Millimeter- and Submillimeter-Waves with Cells and Cell Processes" SPIE Photonics West, BIOS, San Francisco, CA, paper 7562-17, Jan. 2010
- [3] Victor Píkov, Xianghong Arakaki, Michael Harrington, Scott E Fraser and Peter H Siegel "Modulation of neuronal activity and plasma membrane properties with low-power millimeter waves in organotypic cortical slices" *J. Neural Eng.* 7 045003 doi: 10.1088/1741-2560/7/4/045003
- [4] J.P. McNamee, V. Chauhan "Radiofrequency Radiation and Gene/Protein Expression: A Review" *Radiation Research* 172, 265-287 (2009)
- [5] E. R. Adair and D. R. Black, Thermoregulatory responses to RF energy absorption. *Bioelectromagnetics Suppl.* 6, S17-S38 (2003).
- [6] K. R. Foster and R. Glaser, Thermal mechanisms of interaction of radiofrequency energy with biological systems with relevance to exposure guidelines. *Health Phys.* 92, 609-620 (2007).
- [7] ICNIRP Guidelines "Guidelines for Limiting Exposure to Time-varying Electric, Magnetic, and Electromagnetic fields (up to 300 GHz)". *Health Physics* 74 (1998) 494-522.
- [8] E.E. Fesenko, A. Gluvstein, "Changes in the state of water, induced by radiofrequency electromagnetic fields," *FEBS Lett.* v.367, pp.53-55, 1995.
- [9] O.A. Ponomarev, E.Fesenko, "The properties of liquid water in electric and magnetic fields," *Biofizika* v.45, pp.389-398, 2000.
- [10] S.J. Kim, B. Born, M. Havenith and M. Gruebele, "Real time detection of protein dynamics upon protein folding by terahertz absorption spectroscopy," *Angewandte Chemie International Edition*, Wiley Interscience, Engl, v47, pp. 6486-6489, 2008.
- [11] U. Heugen, G.Schwaab, E. Brundermann, M. Heyden, X.Yu, D.M. Leitner and M. Havenith, "Solute-induced retardation of water dynamics probed directly by terahertz spectroscopy," *Proc Natl Acad Sci USA*, v.103, pp.12301-12306, 2006.
- [12] M. Zhadobov et al. "Numerical and Experimental Approaches to Millimeter-Wave Dosimetry for *in vitro* Experiments" Conference on Infrared, Millimeter and Terahertz Waves, 2008. IRMMW-THz 2008. 33rd International 10.1109/ICIMW.2008.4665728

